Int. J. Solids Structures, 1970, Vol. 6, pp. 893 to 908 Pergamon Press. Printed in Great Britain

LIMIT ANALYSIS OF CYLINDRICAL SHELLS WITH LONGITUDINAL RIB REINFORCEMENTS

ANDRÉ BIRON†

École Polytechnique, Montreal, Canada

Abstract—A cylindrical shell is considered with a cross-section composed of two rims, generally of different thicknesses, separated by longitudinal ribs. The yield surface is derived using the strain mapping method for the Tresca yield condition. The collapse pressure is then computed for the case of an open cantilever shell under pressure. It is found that, for this particular problem, there is little savings of material to be made by use of rib reinforcements, but that there may be some savings for other loading and end conditions where axial bending has an important role.

NOTATION

A area between two ribs
a distance between two consecutive ribs
b width of rib
D height of rib
H_1 one half of thickness of inside rib
H_2 one half of thickness of outside rib
$K_x = \dfrac{-\mathrm{d}^2W}{\mathrm{d}X^2}$ longitudinal curvature rate
L length of shell
$M_0 = \sigma_0 H_1^2$ reference yield moment per unit length
M_x average bending moment in the axial direction per unit length
$m = M_x/M_0$
$N_0 = 2\sigma_0 H_1$ reference yield force per unit length
N_x average longitudinal force in the axial direction per unit length
N_ϕ circumferential force per unit length
$n = N_\phi/N_0$
P internal pressure
$p = PR/N_0$
p^* collapse (or yield) pressure
R radius of shell
T average shear force per unit length
$t = T\left(\dfrac{R}{M_0N_0}\right)^{\frac{1}{2}} = \dfrac{T}{\sigma_0 H_1}\left(\dfrac{R}{2H_1}\right)^{\frac{1}{2}}$
W radial velocity, positive inward
$w = W/R$
X axial direction
Z radial direction, measured from the median surface of the inside rim, positive outward
$\alpha = b/a \quad 0 \leq \alpha < 1$
$\beta = D/H_1 \quad 0 \leq \beta < \infty$
$\gamma = H_2/H_1 \quad 0 \leq \gamma < \infty$
ε_x axial strain rate
ε_ϕ average circumferential strain rate
$\varkappa_x = K_x H_{1/2}$

† Associate Professor, Division of Applied Mechanics, Department of Mechanical Engineering.

$\Lambda = L\left(\frac{N_0}{M_0 R}\right)^{\frac{1}{2}} = L\left(\frac{2}{RH_1}\right)^{\frac{1}{2}}$

$\xi = X\left(\frac{N_0}{M_0 R}\right)^{\frac{1}{2}} = X\left(\frac{2}{RH_1}\right)^{\frac{1}{2}}$

σ_0 yield stress of material
σ_x axial stress
σ_ϕ circumferential stress
ϕ circumferential direction

INTRODUCTION

IN THE analysis of the behavior of plates and shells, it is generally assumed that the material is isotropic and that the thickness is uniform. Over the last few years, however, several studies [1–3] have been undertaken on anisotropic structures, produced by an arrangement of isotropic material providing direction-dependent properties, such as in rib-reinforced shells. Some methods in particular have been suggested to establish the yield surface for the plastic analysis of these structures, and it is of interest to examine whether such an arrangement may provide an improvement in the carrying capacity of the shell over results obtained with a uniform thickness, the material volume remaining constant.

The aim of the present work is to evaluate, through limit analysis, how a rib-reinforced design will affect the carrying capacity for a specific problem, that of an open cantilever cylindrical shell subjected to pressure. For this purpose, longitudinal ribs are considered with a cross-section as in Fig. 1. There are two rims, with different thicknesses, $2H_1$ and $2H_2$, separated radially by ribs of height D and width b. The circumferential distance between two consecutive ribs is a. The problem studied in [2] is therefore a special case of the present study where the thickness of the outside rim is zero.

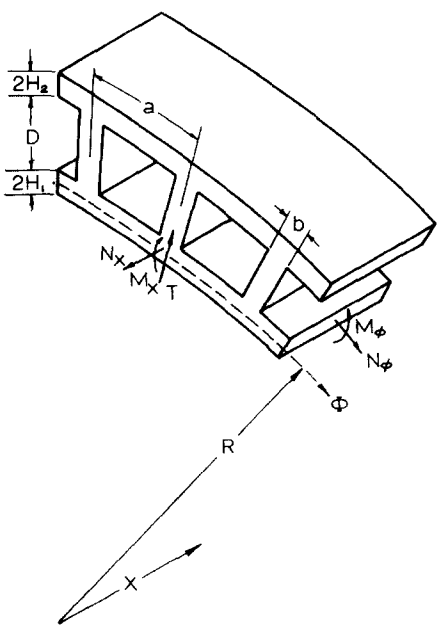

FIG. 1. Shell element.

The geometrical configuration is nonsymmetric, and for the purpose of the analysis must be reduced to a rotationally symmetric problem. We shall therefore consider appropriate average values of the circumferential deformation.

The approach used here is similar to that of [2]. The yield surface is derived using the strain mapping method. Basic equations for cylindrical shells are recalled for use with nonlinear yield conditions. The shell problem is then solved and conclusions are given relative to whatever saving of material, if any, may result from these rib-reinforcements. Other loading conditions are briefly discussed.

FORMULATION OF THE PROBLEM

Let us consider a cylindrical shell with a cross-section as in Fig. 1, where the stress resultants N_x, M_x, N_ϕ, M_ϕ and T and the radial velocity W are shown in the positive direction. The material of the rim and of the ribs is isotropic, incompressible, rigid perfectly plastic with the yield stress σ_0. It is further assumed that this material obeys the Tresca yield condition and that its constitutive equation is that of the plastic potential-flow law.

In order to simplify the presentation, only the case of zero axial force N_x will be considered here. As usual, the influence of the transverse shear T on yielding is neglected, and the circumferential bending moment M_ϕ is not a generalized stress since the mean circumferential curvature rate is zero. Hence the yield surface may be expressed in dimensionless form in terms of two stresses only, namely the circumferential force n and the average axial bending moment m.

CONSTRUCTION OF THE YIELD SURFACE

The yield surface is obtained from the usual assumption of straight normals and from the strain mapping method suggested by Onat and Prager [4], which is a consequence of the plastic potential-flow law.

The Tresca criterion is expressed in terms of stresses σ_x and σ_ϕ [Fig. 2(a)].

$$\max\{|\sigma_x|, |\sigma_\phi|, |\sigma_x - \sigma_\phi|\} \leq \sigma_0. \tag{1}$$

The plastic potential-flow law may be described in terms of a stress point (σ_x, σ_ϕ) and a strain-rate vector $(\varepsilon_x, \varepsilon_\phi)$. For a non-zero vector, the corresponding stress point on surface (1) must be such that the angle between this vector and any other vector inside the surface is at least a right angle, the strain-rate vector being directed outwards.

It is thus possible, from any given distribution of ε_x and ε_ϕ, to deduce the distribution of σ_x and σ_ϕ, and therefore to compute the generalized stresses. If, for example, ε_x and ε_ϕ are both positive, the corresponding stress point must be at corner B of the yield hexagon. In this fashion, each of the six regions of Fig. 2(b) corresponds to a corner of the hexagon, and the lines separating these regions correspond to the sides.

To obtain the yield surface in terms of the generalized stresses, it is necessary to consider all possible combinations of distributions of ε_x and ε_ϕ, ε_ϕ being distributed uniformly across the rims.

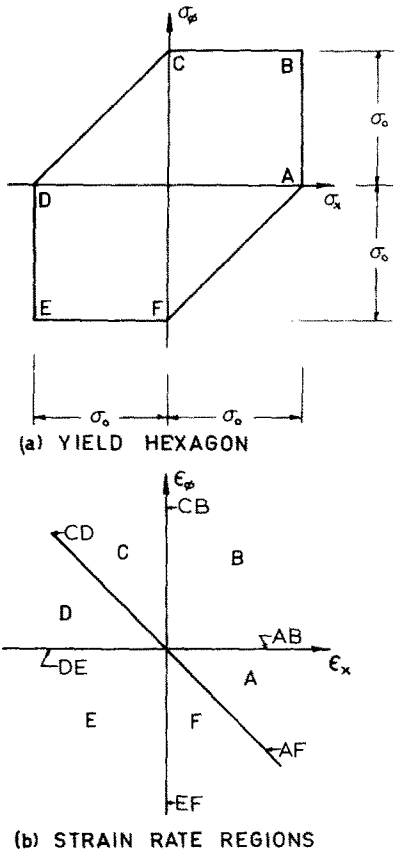

FIG. 2. Tresca yield curve and associated strain rates.

In the ribs, the state of stress is uniaxial in the X direction. In the rims, at a distance Z from the median surface of the inside wall, the sign of ε_x and ε_ϕ and their relative values are considered. Using Fig. 2, the stress distribution is then obtained.

In order to construct the entire yield surface, a total of fifteen cases must be studied. Let us examine one case in detail, that of case 3 shown in Fig. 3, where two parameters r and j are used to describe the strain rate distribution.

(a) For $Z > H_1 + D + (1+j)H_2$, $\varepsilon_\phi < 0$, $\varepsilon_x > 0$, $|\varepsilon_x| > |\varepsilon_\phi|$. This corresponds to corner A of the yield hexagon in Fig. 2, and therefore in this region $\sigma_x = \sigma_0$, $\sigma_\phi = 0$.

(b) For $H_1 + D < Z < H_1 + D + (1+j)H_2$, $\varepsilon_\phi < 0$, $\varepsilon_x > 0$, $|\varepsilon_x| < |\varepsilon_\phi|$. This corresponds to corner F, and $\sigma_x = 0$, $\sigma_\phi = -\sigma_0$.

(c) For $H_1 + rD < Z < H_1 + D$, $\varepsilon_x > 0$ and, since the state of stress is uniaxial, $\sigma_x = \sigma_0$.

(d) For $H_1 < Z < H_1 + rD$, $\varepsilon_x < 0$, thus $\sigma_x = -\sigma_0$.

(e) For $-H_1 < Z < H_1$, $\varepsilon_x < 0$, $\varepsilon_\phi < 0$. This corresponds to corner E of the hexagon and $\sigma_x = \sigma_\phi = -\sigma_0$.

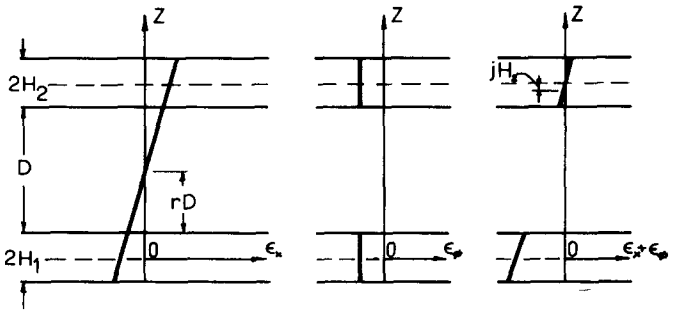

FIG. 3. Typical strain rate and stress distribution (Case 3).

The stress distribution is thus as illustrated in Fig. 3(b), and the stress resultants are:

$$
\begin{aligned}
N_x &= \frac{1}{a}\int_A \sigma_x \,\mathrm{d}A = [(1-j)H_2 a + (1-2r)Db - 2aH_1]\sigma_0/a \\
-M_x &= \frac{1}{a}\int_A \sigma_x Z \,\mathrm{d}A = \left\{(1-j)H_2 a\left[H_1 + D + \frac{(3+j)}{2}H_2\right]\right. \\
&\qquad \left. + (1-2r)DbH_1 + \frac{(1-2r^2)}{2}D^2 b\right\}\sigma_0/a \\
N_\phi &= \int_{-H_1}^{H_1} \sigma_\phi \,\mathrm{d}Z + \int_{H_1+D}^{H_1+D+2H_2} \sigma_\phi \,\mathrm{d}Z = -[(1+j)H_2 + 2H_1]\sigma_0 .
\end{aligned}
\tag{2}
$$

The axial force N_x being zero, a relation is easily derived between parameters r and j:

$$
r = \frac{1}{2} - \frac{[2-(1-j)\gamma]}{2\beta\alpha} \tag{3}
$$

where

$$
\alpha = b/a \qquad \beta = D/H_1 \qquad \gamma = H_2/H_1 . \tag{4}
$$

The following inequalities related to parameters r and j must be satisfied:

$$
\begin{aligned}
0 \le r \le 1 \\
-1 \le j \le 1 .
\end{aligned}
\tag{5}
$$

Thus, from (3) and (5), we obtain the following limits for parameter j:

(a) If $\beta\alpha < 2$

(1) If $\beta\alpha - 2\gamma < -2$

$$1 - \frac{(\beta\alpha + 2)}{\gamma} \leq j \leq 1 - \frac{(2 - \beta\alpha)}{\gamma}. \tag{6a}$$

(2) If $\beta\alpha - 2\gamma \geq -2$

$$-1 \leq j \leq 1 - \frac{(2 - \beta\alpha)}{\gamma}. \tag{6b}$$

(b) If $\beta\alpha \geq 2$

(1) If $\beta\alpha - 2\gamma < -2$

$$-1 - \frac{(\beta\alpha + 2)}{\gamma} \leq j \leq 1. \tag{6c}$$

(2) If $\beta\alpha - 2\gamma \geq -2$

$$-1 \leq j \leq 1. \tag{6d}$$

The generalized stresses may therefore be written in terms of one parameter j from (2)–(4):

$$\begin{aligned} n &= -\frac{(1+j)\gamma}{2} - 1 \\ -m &= 2 - \frac{[2-(1-j)\gamma]^2}{4\alpha} + \frac{[2+(1-j)\gamma]\beta}{2} + \frac{\beta^2\alpha}{4} + (1-j^2)\gamma^2 + \frac{(1-j)^2\gamma^2}{2} \end{aligned} \tag{7}$$

where

$$n = \frac{N_\phi}{2\sigma_0 H_1} \qquad m = \frac{M_x}{\sigma_0 H_1^2} \tag{8}$$

and where the allowed values of j are given by equations (6)

Equations (7) define in parametric form one part only of the yield surface. All other fourteen cases of strain rate distributions are studied in the same manner.

It turns out, from the overall analysis, that different cases are applicable depending on the sign of the following four inequalities:

$$\begin{aligned} \beta\alpha &\lessgtr 2 \\ \beta\alpha + 2\gamma &\lessgtr 2 \\ \beta\alpha - 2\gamma &\lessgtr 0 \\ \beta\alpha - 2\gamma &\lessgtr -2. \end{aligned} \tag{9}$$

The functions given in (9) divide a $\beta\alpha$ vs. 2γ plane into eight different regions, as shown in Fig. 4, and a different yield surface corresponds to each region as indicated in Tables 1–8 of [5].

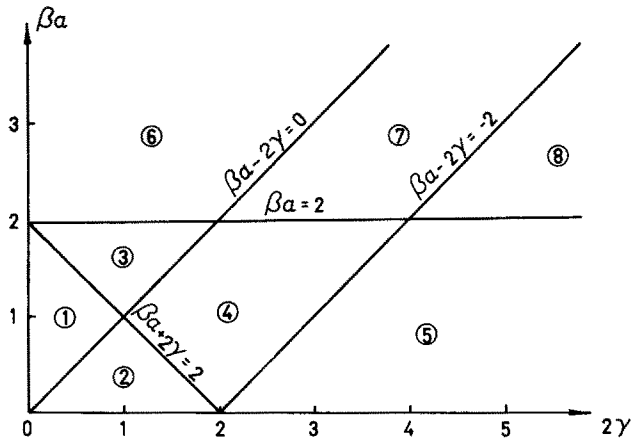

FIG. 4. Regions of study.

The shape of the yield surface depends on the region of Fig. 4. Typical curves are given in Figs. 5(a)–5(h) for $\alpha = 0{\cdot}5$ and for different values of β and γ corresponding to each of the eight regions of reinforcement. Circled numbers correspond to cases referred to in the tables.

It is noted that this method gives rise to a discontinuity of deformation in the circumferential direction, at the interface of the rim and the rib. Thus, for complete solutions, the present theory should be restricted to small values of α. Otherwise, the yield surface constitutes a lower bound.

BASIC EQUATIONS FOR THE ANALYSIS OF CYLINDRICAL SHELLS

The solution of the limit analysis problem of a cylindrical shell implies the integration of equilibrium equations combined with the yield condition. For a uniform cross-section, the sandwich shell approximation to the yield surface is generally used and, since it is linear, the integration can be carried out without difficulty.

For the problem of rib-reinforced shells, however, the yield surface as developed with the present method is nonlinear. In this case, a different approach is desirable and has been suggested in [2]. Some details of the development must be reproduced here for completeness.

The equations of equilibrium for a cylinder under pressure are:

$$m' = t \tag{10}$$

$$t' + n = p \tag{11}$$

where primes indicate differentiation with respect to the dimensionless axial coordinate ξ, p is the dimensionless pressure and t is the dimensionless shear force per unit length. Introducing the parameter s used to express the yield condition, the following relations

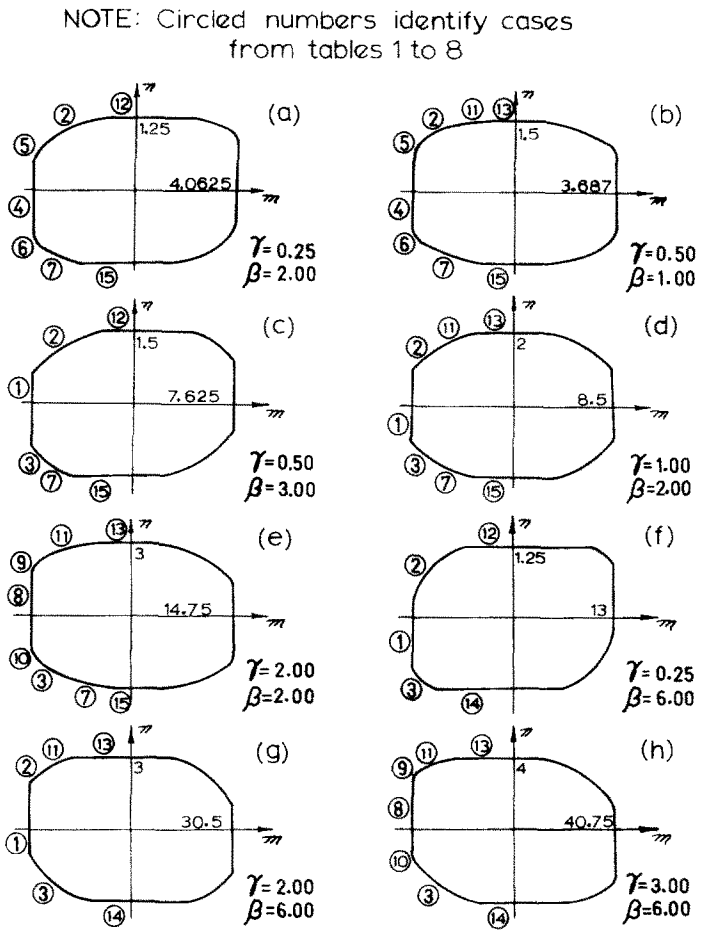

FIG. 5. Typical yield surfaces for $\alpha = 0{\cdot}5$ and various values of β and γ.

may then be easily obtained from (10) and (11):

$$t^2 = 2\int_{s_0}^{s}(p-n)\frac{\mathrm{d}m}{\mathrm{d}s}\,\mathrm{d}s + t^2(s_0) \tag{12}$$

$$\xi = \int \frac{1}{t}\frac{\mathrm{d}m}{\mathrm{d}s}\,\mathrm{d}s. \tag{13}$$

Thus substituting $\xi = \Lambda$, the shell length, in (13), a relation between this length and the yield pressure is obtained.

Regarding kinematic admissibility, the following strain rate–velocity relations are valid from [6]:

$$\begin{aligned} \varepsilon_\phi &= -w \\ \varkappa_x &= -w'' \end{aligned} \tag{14}$$

where w is the dimensionless radial velocity.

The plastic potential-flow law requires that the flow vector $(\varepsilon_\phi, \varepsilon_x)$ be normal to the yield surface $\Phi(n, m) = 0$. Thus:

$$m'w'' + n'w = 0. \tag{15}$$

Using (10), (11) and the fact that p is constant

$$\left(\frac{w}{t}\right)' = \frac{w't - wt'}{t^2} = \frac{G}{t^2} \tag{16}$$

and finally, from (13):

$$w = Gt \int \frac{1}{t^3}\left(\frac{dm}{ds}\right) ds + Kt \tag{17}$$

where G and K are constants of integration.

Therefore, to prove that a given stress profile corresponds to the exact solution, it is sufficient to show that w in (17) is of the proper sign, corresponding to an outer normal to the yield surface, and that it satisfies the boundary conditions.

SOLUTION OF PROBLEM: A CANTILEVER CYLINDER UNDER PRESSURE

To evaluate the effect of rib reinforcement on the load carrying capacity under constant material volume, we examine the problem which has been solved for $\gamma = 0$ in [2], that of an open-ended cantilever shell under constant pressure, as shown in Fig. 6. This may be considered as an application of limit analysis to the study of a reinforced nozzle.

A different study must be made for each of the eight regions shown in Fig. 4. We shall consider in some detail one example for geometry parameters corresponding to region No. 1, i.e.

$$\begin{aligned} \beta\alpha + 2\gamma &\leq 2 \\ \beta\alpha - 2\gamma &\geq 0. \end{aligned} \tag{18}$$

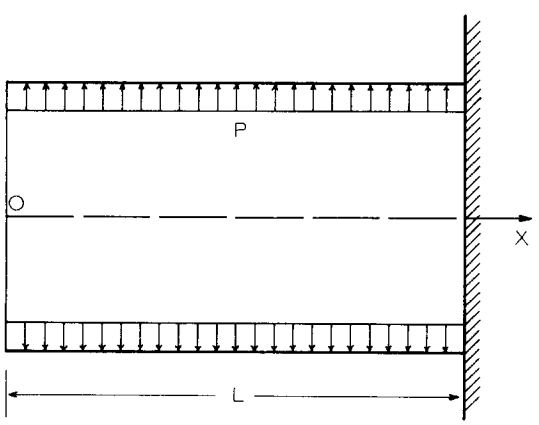

FIG. 6. Longitudinal section of cantilever shell.

It is reasonable to expect that both w and w'' will be negative throughout the shell, hence from (14), that both strain rate components will be positive. Thus the assumed stress profile is as shown in Fig. 7 and the portion of the yield surface which must be considered corresponds to cases 15, 7 and 6.

The boundary conditions are:

$$\begin{aligned} &\text{At} && \xi = 0 && m = 0 \\ & && && t = 0 \\ & && && w = -w_0. \\ &\text{At} && \xi = \Lambda && w' = 0 \quad \text{or} \quad m = m_{\max} \\ & && && w = 0 \end{aligned} \tag{19}$$

and the quantities m, n, t, w and w' are necessarily continuous at $\xi = \bar{\xi}$ and $\xi = \bar{\bar{\xi}}$.

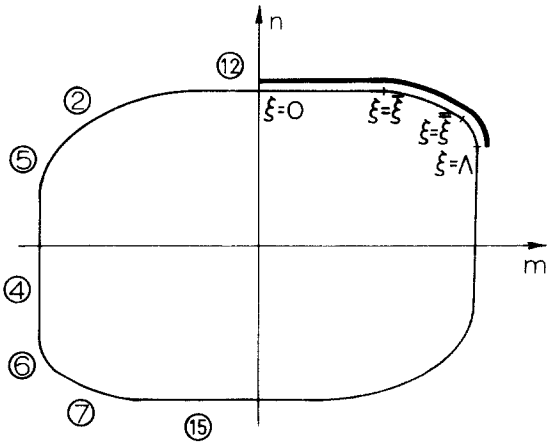

FIG. 7. Stress profile for cantilever shell problem.

The relation between the axial distance ξ and the yield pressure p^* may then be obtained from (12) and (13). If we choose the boundary condition $m = m_{\max}$ at $\xi = \Lambda$, a selection which will be confirmed later, we obtain a direct relation between the shell length Λ and the yield pressure p^*, involving only an integration which in general must be carried out numerically.

It remains to be shown that the selected stress profile and the selected boundary condition at $\xi = \Lambda$ are correct.

It will be seen that in all cases the yield pressure is such that

$$p^* > n_{\max} = \gamma + 1. \tag{20}$$

Hence, from (11) and (20), $t' > 0$. From boundary condition (19), w is negative and t is zero at the free end. Thus, from (16), constant G is positive, and therefore:

$$\left(\frac{w}{t}\right)' > 0 \tag{21}$$

holds throughout the shell. Since the denominator t increases as ξ increases, w must be a monotonically increasing function of ξ. At $\xi = \Lambda$, $w = 0$. Thus, w cannot be positive, and from (21), (16), w' cannot be zero at $\xi = \Lambda$. We conclude that the velocity is of the proper sign, and that the boundary condition $m = m_{\max}$ at the fixed end is the only possible choice. The solution is kinematically admissible, and therefore complete.

The general form of the relation between the shell length and the pressure may be expressed as follows:

$$\Lambda = \bar{\xi} - \sum_{i=7,6,3,10} g_i \int_{\theta_i}^{\phi_i} \left\{ F^i(s) - F^i(\phi_i) + t_i^* \right\}^{-\frac{1}{2}} (a_i - b_i s)\, \mathrm{d}s \tag{22}$$

where:

$$F^n(u) = 2\left\{ c_n a_n u - (a_n d_n + b_n c_n)\frac{u^2}{2} + b_n d_n \frac{u^3}{3} \right\}. \tag{23}$$

Values of terms in (22) and (23) are given in Tables 9 and 10 of [5]. This particular form of solution can be easily formulated on a digital computer by assuming a value of p^*. The corresponding shell length Λ is then obtained.

A different set of curves must of course be presented for any combination of the three parameters α, β, γ. A simpler, although slightly approximate, method of providing results for the present problem may be based on the observation in [2] that, with $\gamma = 0$, all curves would practically coincide if the collapse pressure were replotted as a function of $\bar{\Lambda}$, where:

$$\bar{\Lambda} = L\left(\frac{N_0}{RM_{\max}}\right)^{\frac{1}{2}} = \frac{\Lambda}{\sqrt{m_{\max}}}. \tag{24}$$

The maximum moment can easily be established as follows:

(a) If $(\beta\alpha + 2\gamma) \leq 2$

$$m_{\max} = 1 + \beta\alpha(1-\gamma) + \frac{\beta^2\alpha}{2} - \frac{\beta^2\alpha^2}{4} + \gamma(2 + 2\beta + \gamma). \tag{25a}$$

(b) If $(\beta\alpha + 2\gamma) > 2$

(1) If $\beta\alpha - 2\gamma \geq -2$

$$m_{\max} = 2 - \frac{(1-\gamma)^2}{\alpha} + \beta(1+\gamma) + \frac{\beta^2\alpha}{4} + 2\gamma^2. \tag{25b}$$

(2) If $\beta\alpha - 2\gamma < -2$

$$m_{\max} = \gamma^2 + (\beta\alpha + 2)\gamma + 1 + \frac{\beta^2\alpha}{2} - \frac{\beta^2\alpha^2}{4} + 2\beta - \beta\alpha. \tag{25c}$$

It is therefore possible to present results with very little error for all cantilever shells as in Fig. 8, with a particular curve for each value of γ. The corresponding equation is approximately:

$$\bar{\Lambda} \simeq \left(\frac{2}{p^* - \gamma - 1}\right)^{\frac{1}{2}}. \tag{26}$$

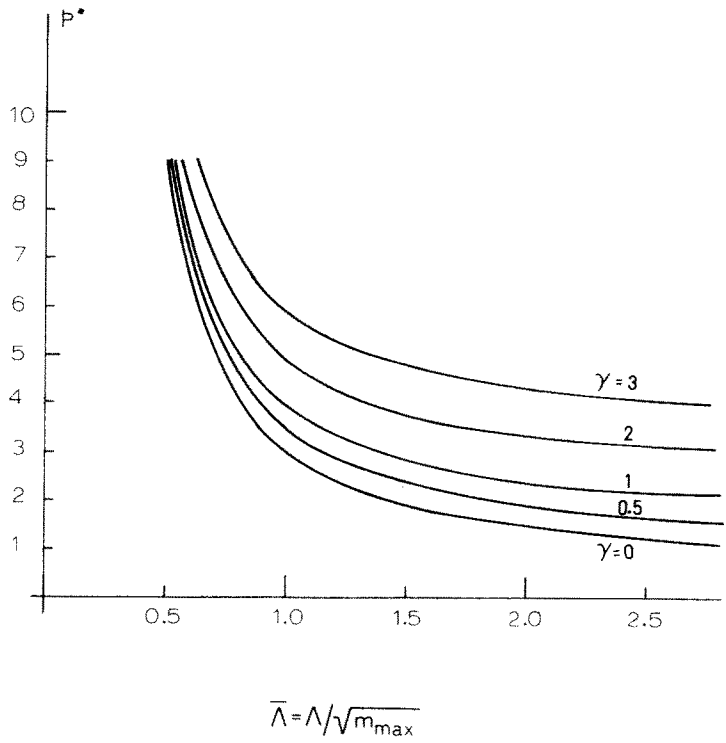

FIG. 8. Approximate relation between collapse pressure and shell length for cantilever shells.

COMPARISON OF COLLAPSE PRESSURES, CONSTANT VOLUME AND LENGTH

In order to evaluate the actual improvement, if any, which can be obtained from a rib-reinforced shell, the cantilever shell sample problem may be considered by comparing the results to those of a uniform shell of the same physical length L. Then, for a constant amount of material, it is possible to find the collapse pressure ratio for any combination of parameters α, β and γ.

It can easily be shown that, for equal physical lengths and equal volumes, we must have the following relation between dimensionless shell lengths Λ_1 and Λ_2:

$$\Lambda_1 = \frac{\Lambda_2}{(1+\gamma+\beta\alpha/2)^{\frac{1}{2}}} \tag{27}$$

and that the ratio of physical collapse pressures P_1^* and P_2^* is, in terms of dimensionless quantities:

$$\frac{P_2^*}{P_1^*} = \frac{p_2^*}{p_2^*(1+\gamma+\alpha\beta/2)} \tag{28}$$

where subscripts 1 and 2 refer to uniform and rib-reinforced shells respectively.

The comparison is then carried out as follows: from selected values of the physical quantities, the "equivalent length" for a uniform shell of radius R and thickness $2H$ is

$$\Lambda_1 = \frac{L\sqrt{2}}{\sqrt{(RH)}}. \tag{29}$$

The dimensionless collapse pressure for the uniform shell p_1^* is obtained from [2]†. For given parameters α, β, γ, the corresponding dimensionless length Λ_2 for the rib-reinforced shell is obtained from (27) and the dimensionless collapse pressure p_2^* is given by the present solution. The pressure ratio P_2^*/P_1^*, from (28), is shown in Fig. 9 as a function of Λ_1.

An optimum choice of values for α and β must be guided by physical considerations, since theoretically α should be as small as possible and β should be rather large. Values given in Fig. 9 are probably reasonable if the number of ribs is not too large. The only practical "optimum" guidance from the present analysis is related to γ, for which a value of approximately 0·75 yields the best results.

It is noted that there is some improvement in the collapse pressure for rib-reinforced

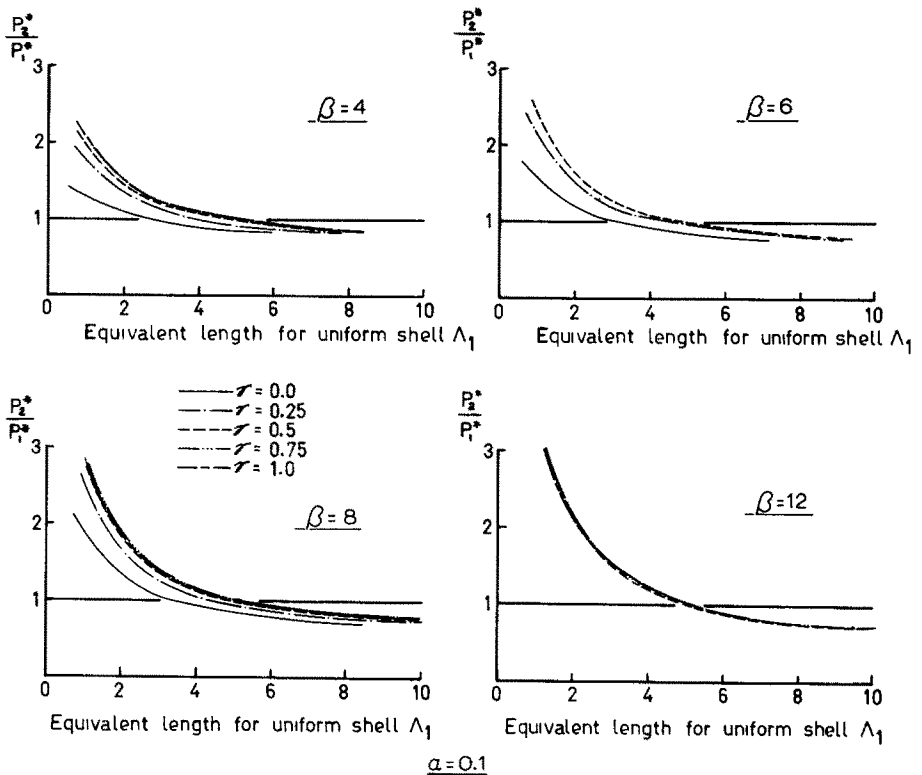

FIG. 9. Comparison between rib-reinforced and uniform cantilever shells for constant length and volume.

† There is a misprint in the published solution and one should read: $\psi = \sin^{-1}\left\{\frac{-\gamma_3}{1-\gamma_3}\right\}^{\frac{1}{2}}$.

shells only for values of Λ_1 smaller than approximately 5, corresponding to very short shells of length slightly less than the radius.

OTHER LOADING CONDITIONS

It is clear from Fig. 9 that, from the point of view of economy of material, there is no advantage in using longitudinal ribs for the present problem of an open cantilever cylinder subjected to pressure, unless the length is extremely small as in a ring. A possible explanation for this is that the response here is almost that of a pure membrane for $L \gtrsim R$, and that the beneficial effect of the axial moment on the limit load is no longer significant.

For very short shells, however, there was an increase in the carrying capacity which was appreciable. While this has little practical consequence for a nozzle, it suggests that for other loading conditions where axial bending has an important role, a design with longitudinal ribs might prove beneficial.

An example which may be of interest in this respect is the problem of a circumferential ring of pressure of intensity $2F$ on a shell whose ends are restrained against rotation. Without carrying out the detailed study, it is possible to make a rough evaluation of the order of magnitude of the increase in carrying capacity which could be generated by a rearrangement of a constant amount of material as in Fig. 1.

Let us first establish an upper bound on this increase by using a rectangular "limited interaction" yield surface which circumscribes the exact surface, thus with maximum values $n_{\max}(=\gamma+1)$ and $m_{\max}$. From the analysis in [6], the collapse load is then

$$F_2 = 2\left(\frac{M_{\max} N_{\max}}{R}\right)^{\frac{1}{2}} \tag{30}$$

if the shell length is at least of the order of the radius. Comparing with the uniform Tresca collapse load F_1 for a uniform shell of the same material volume from [6, 7], an upper bound to the collapse load ratio is:

$$\left(\frac{F_2}{F_1}\right)^{+} = \frac{2}{1{\cdot}826} \frac{(\gamma+1)^{\frac{1}{2}} m_{\max}^{\frac{1}{2}}}{(1+\gamma+\alpha\beta/2)^{\frac{3}{2}}} \tag{31}$$

where $m_{\max}$ is given in equations (25).

Similarly, by inscribing a rectangular yield surface of maximum values $n'_{\max}$ and $m_{\max}$, we obtain a lower bound:

$$\left(\frac{F_2}{F_1}\right)^{-} = \frac{2}{1{\cdot}826} \frac{(n'_{\max})^{\frac{1}{2}} m_{\max}^{\frac{1}{2}}}{(1+\gamma+\alpha\beta/2)^{\frac{3}{2}}}. \tag{32}$$

Figure 10 shows the variations of the upper bound $(F_2/F_1)^+$ for the geometrical parameters of Fig. 9. It is of interest to observe that the optimum value of γ is approximately 0·75, as in the reinforced nozzle problem. For this value of γ, the lower bound $(F_2/F_1)^-$ is also given. These bounds are of course very far apart, and the exact solution could easily be obtained, if required, through a numerical integration using the yield surface presently developed and the general relation in [7]. This is not necessary here, as the bounds are sufficient to show that an appreciable increase in the carrying capacity (between 38 per cent and 110 per cent for $\beta = 12$) may be obtained by a suitable rearrangement of the material for the problem of a circumferential ring of pressure.

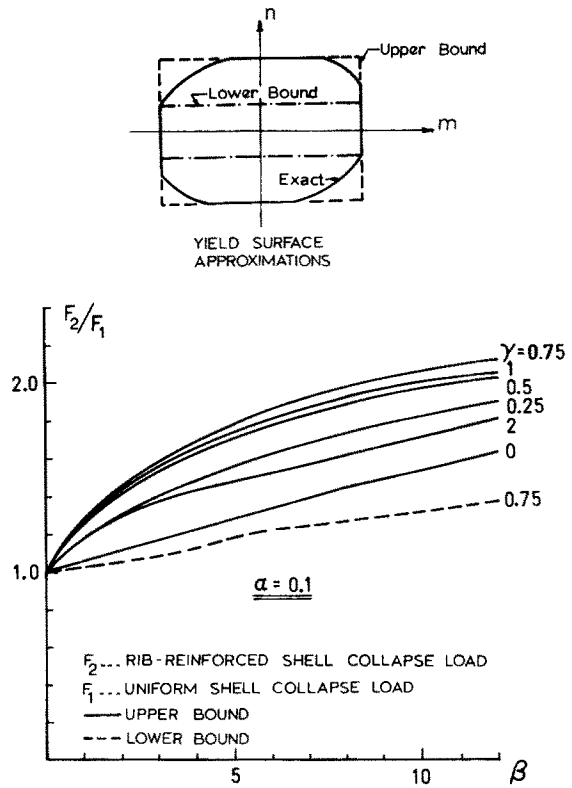

FIG. 10. Bounds on collapse load ratios for circumferential pressure ring, with constant volume of material.

CONCLUSION

A method for the limit analysis of rib-reinforced cylindrical shells as shown in Fig. 1 has been proposed. The yield surface has been derived and the problem of an open cantilever shell subjected to pressure has been solved in detail.

The comparison of rib-reinforced shells with uniform shells of the same material volume has shown that for the open cantilever shell problem there is little savings of material to be gained by longitudinal rib-reinforcements mostly because of the negligible effect of axial bending. It appears likely, however, that an increase in the carrying capacity may be obtained for loading conditions such that axial bending has a predominant role, as was observed for the circumferential ring of pressure example. An optimum arrangement of Fig. 1 would be such that the outer rim thickness is approximately $\frac{3}{4}$ of that of the inner rim.

Acknowledgement—The present study is part of a project sponsored by the National Research Council of Canada, Grant No. A-4109. The author wishes to mention the contribution of C. Hubert and G. Matton who carried out many of the computations, and of Professor A. Sawczuk of the Polish Academy of Sciences for his valuable comments.

REFERENCES

[1] Y. V. NEMIROVSKY and YU. N. RABOTNOV, Limit analysis of ribbed plates and ribbed shells, *Non-Classical Shell Problems*, pp. 786–807. North Holland (1964).
[2] A. BIRON and A. SAWCZUK, Plastic analysis of rib-reinforced cylindrical shells. *J. appl. Mech.* **34**, 37–42 (1967).
[3] YU. V. NEMIROVSKY, Limit analysis of cylindrical waffle shells (in Russian). *Inz. Z. Mekh. Tverdogo Tela* 3, 52–59 (1967).
[4] E. T. ONAT and W. PRAGER, Limit analysis of shells of revolution. *Proc. Netherlands Acad. Sci.* **B57**, 334–348 (1954).
[5] A. BIRON, An evaluation of the carrying capacity of some rib-reinforced cylindrical shells. Report No. 1767 Division of Applied Mechanics, École Polytechnique, Montreal.
[6] P. G. HODGE, JR., *Plastic Analysis of Structures.* McGraw-Hill (1959).
[7] A. SAWCZUK and P. G. HODGE, JR., Comparison of yield conditions for circular cylindrical shells. *J. Franklin Inst.* **269**, 362–374 (1960).

(*Received* 2 *July* 1969; *revised* 13 *October* 1969)

Абстракт—Обсуждается цилиндрическая оболочка с поперечным сечением, состоящим из двух опорных колец, разной толщины, разделенных продольными ребрами. Определяется поверхность течения, используя метод отображения для условия текучести Трески. Определяется, затем, давление разрушения для случая открытой консольной оболочки под давлением. В этом особом случае, констатируется малая экономия материала при использовании усиления ребрами, одноко можно получить некоторую экономию для других нагрузок и краевых условий, где осевой изгиб играет важную роль.